

PAPER • OPEN ACCESS

Study on the volute chamber shape of swirling shaft adopted in water diversion project

To cite this article: Yang Li *et al* 2019 *IOP Conf. Ser.: Earth Environ. Sci.* **227** 042033

View the [article online](#) for updates and enhancements.



IOP | ebooks™

Bringing you innovative digital publishing with leading voices to create your essential collection of books in STEM research.

Start exploring the collection - download the first chapter of every title for free.

Study on the volute chamber shape of swirling shaft adopted in water diversion project

Yang Li¹, Rongbin Zhang², Lei Yang^{1,4}, Pengpeng Han³, Yisen Wang¹ and Chang Xu¹

¹ State Key Laboratory of Water Resources and Hydropower Engineering Science, Wuhan University;

² Yunnan Institute of Water & Hydropower Engineering Investigation, Design and Research;

³ China Communications Construction Company Second Harbour Engineering Company LTD.

⁴ Email: lylshow@whu.edu.cn

Abstract. As an environment-friendly internal energy dissipation technology, the swirling shaft energy dissipation has been more and more applied. In this paper, the influence of the shape of the volute chamber on the flow pattern and energy dissipation rate is studied by the CFD numerical simulation method combined with the physical model test method. The results show that with the increasing of the diameter of the volute chamber, the diameter of the cavity in the volute chamber increases correspondingly, which effectively alleviates the backwater phenomenon on the upstream channel section of the shaft. Increasing the width of the inlet of the volute chamber can promote the flow pattern of the upstream channel section from the pressure flow to the non-pressure flow. The setting of the arc wedge rectification flip bucket can improve the inlet and inner flow pattern of the volute chamber.

1. Introduction

A series of energy dissipation measures are often required for the discharge of hydraulic structures in alpine and gorge region. Reconstructing the existing construction diversion tunnel into the swirling shaft flood discharge tunnel can not only meet the flood discharge requirements, but also reduce the project cost and improve the project efficiency. It has been adopted in Xiluodu hydropower station[1], Gongboxia hydropower station[2] and Shapai hydropower station[3]. After the introduction of the eco-friendly concept, the impact of water conservancy and hydropower projects on the ecological environment has become one of the constraints of engineering feasibility[4]. As an eco-environment-friendly internal energy dissipation technology, due to its small impact on the environment, the quantities and construction difficulty of project are controllable, the energy dissipation rate in the shaft is high, the swirling shaft is also adopted more and more in the water diversion project.

The development of the swirling shaft originated in the 1950s. In order to solve the problem of water flow rotation in the volute shaft discharge tunnel, systematic model tests were conducted by C. Drioli and D. Jeanpierre[5-6]. It indicated that the water flow can enter the volute chamber smoothly, and the water flow in the flat section of the volute chamber belongs to the subcritical flow. Qian Xiaoyan, Deng Jun[7] and other authors focused on the shape of the inlet and outlet of the volute chamber, and analyzed the corresponding flow characteristics and energy dissipation effects of



different shapes of small flip bucket; Dong Xinglin, Guo Jun et al[8] proposed that the negative pressure is easy occurred in the top of the connection section between the inlet and the shaft of the volute chamber, and the negative pressure can be eliminated by adopting the baffle to reduce the flow velocity in the inlet of volute chamber; Gou Fangrong and Huang Huang[9] designed the gate at the inlet of swirling shaft and the flow pattern of the water flow is controlled by adjusting the gate opening. By comparing the discharge coefficient under different gate opening with different discharge capacity, another idea of the optimization scheme of the inlet is proposed. Based on the combination method of model test and numerical simulation, Chen Huayong[10] conducted the comparison and analysis of the measured and calculated results on the important hydraulic parameters, such as water surface line, the remaining height of cross section, the pressure of shaft, the velocity of shaft wall and the energy dissipation rate of the swirling shaft, Niu Zhengming[11] discussed some issues of simulating the swirling shaft with the numerical method, such as applicability of the turbulence model, the division of the grid and the reasonable selection of boundary conditions. Previous studies focused more on the energy dissipation of large-scale hydropower projects, and the study of swirling shaft adopted in water diversion works is few. In this paper, based on the actual water diversion project in Yunnan province, the relationship between the hydraulic characteristics and the body type parameter is analyzed by the combination method of model test and numerical simulation[12-13].

2. Project overview

The Dianzhong water diversion project is a strategic foundation project for sustainable development in Yunnan province, with significant economic, social and ecological benefits. The Qujiang energy dissipation power station is located at the stake mark YH74+755.751m of the water transmission line. The forebay of the power station is connected to the Luofengshan tunnel. The tailwater building is composed of the tailwater shaft and the tailwater pool, followed by the Qujiang inverted siphon. The sluiceway of forebay is connected to the side weir chute in the inlet and the tailwater pool of the power station in the outlet. The design discharge is $20\text{m}^3/\text{s}$ and the total length is 560m. It is located on the ridge between the forebay and the powerstation plant. The swirling shaft is adopted in the energy dissipation of this sluiceway.

The sluiceway consists of upstream channel section, volute chamber section, shaft section, energy dissipation well section and downstream adit section. The upstream channel section is composed of chute section, straight line section 1, curve section, straight line section 2, transition section and entrance section of volute chamber. The starting point elevation of the chute section is 1799.400m and the width is 2.0m; the width of straight line section 1, curve section and straight line section 2 is also 2.0m, the elevation reduces from 1773.566m to 1771.562m, the width of transition section changes from 2.0m to 1.0m, and the bottom elevation is 1771.562m. The length of inlet section of the volute chamber is 10m, and the top elevation of the volute chamber is 1775.562m, the lower elevation is 1770.762m, according to the preliminary test, it is determined that the diameter is 2.5m. The lower part of the volute chamber is connected with the shaft by transition section with the length 3m. The shaft diameter is 2.0m. The bottom elevation of energy dissipation well is 1654.399m. The bottom elevation of inlet and outlet of adit section is 1656.364 and 1653.434m respectively. Figure 1 shows the schematic overall layout and profile of sluiceway with stake mark. (the starting point of the sluiceway is the station number 0+000.000m).

The preliminary design confirmed that the diameter of the volute chamber was 2.5 m. On this basis, four kinds of body type schemes with the diameter D of the volute chamber and the inlet width l of entrance section of the upstream channel section are proposed, and the variation of hydraulic characteristics and the effect on the energy dissipation are studied by numerical simulation. Data in Table 1 show the different parameters adopted in numerical simulation.

The boundary conditions of calculation are as follows: the upstream water level of inlet of chute section is 1801.760m, the designed discharge is $20\text{m}^3/\text{s}$; the water depth of inlet of downstream adit section is 1.86m.

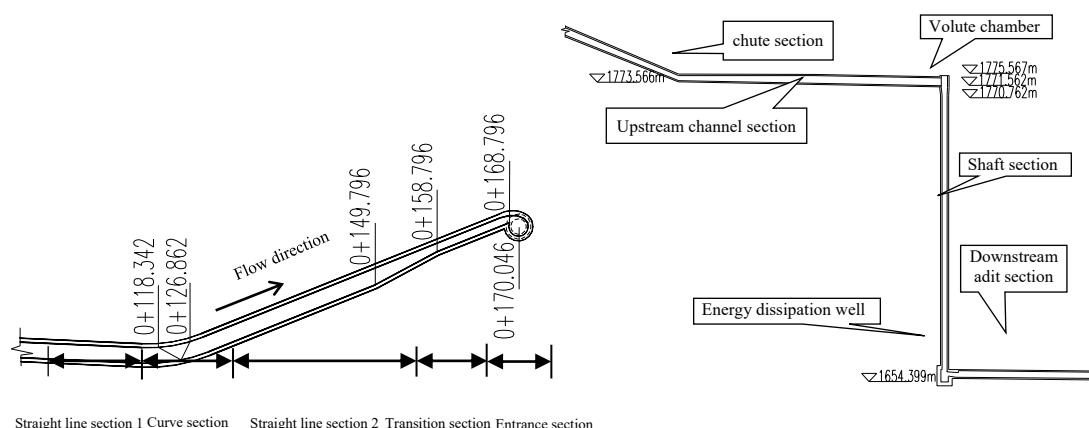


Figure 1. Schematic overall layout of sluiceway.

Table 1. Different combination scheme of volute chamber body type.

Scheme	Diameter D (m)	Inlet width l (m)
1	2.5	1.0
2	3.0	1.0
3	3.0	1.2
4	3.0	1.5

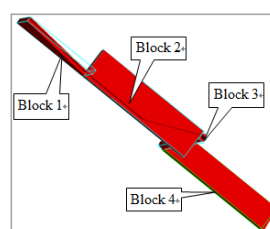


Figure 2. Sluiceway meshing.

3. Mathematical model and simulation results

3.1. Meshing

In the numerical simulation process of the swirling shaft, the calculation grid should be divided according to the variation law of the spiral water flow inside the shaft. For a swirling shaft, a dense mesh unit is required at the intersection of the shaft wall and the water-air interface to accurately simulate the pressure gradient and capture the free surface. According to the structural characteristics of the calculation model, the calculation area is divided into four calculation areas by structured orthogonal grid. Figure 2 shows the specific division of sluiceway. Since the shaft section (block 3) is the main research object and the structure is relatively complex, its mesh size is smaller than other grid sizes, after comparing the accuracy of different size meshes, it's determined to be 0.14m×0.14m×0.14m; The grid size of block 1, block 2 and block 4 is 0.22m×0.22m×0.22m; the total number of grids is 4.54 million, and the number of fluid grids is about 1.64 million.

3.2. Flow pattern analysis

The numerical simulation results show that in scheme 1, a pressure flow is formed at a long distance in front of the curve section. In the volute chamber, the water flow forms a stable cavity, and there is no "choking" phenomenon at the transition section of the shaft entrance. The spiral flow rotates adherence the wall and flows downward. In the whole structure, there is no obvious unfavorable flow pattern such as water flow voiding and discontinuity; in scheme 2, as the diameter of the volute chamber increases, the obstruction in the inlet of the volute chamber is reduced due to the gradually increasing of the pitch of the swirling flow in the volute chamber. Therefore, the length of the pressure flow in upstream channel section of the shaft is reduced. A full section flow is formed in the middle of the curve section of the upstream channel section. The highest elevation of water surface in volute chamber is 1757.78m, which reduced about 1.5m compared with scheme 1. In scheme 3, with the increasing of the width of the entrance section of the volute chamber, the pressure flow is formed 10m before the entrance of the volute chamber. In the scheme 4, the flow pattern in upstream channel

section is no-pressure flow. The highest elevation of water surface in volute chamber is 1757.78m. Compared with the scheme mentioned above, the flow near the center of the volute chamber directly hits on the wall of the volute chamber. The flow is not directed by the walls of the volute chamber, and stable spiral flow cannot be formed in the volute chamber. Although a shaft cavity is formed, the cavity is not stable. Figure 3 shows the flow pattern of all scheme under design discharge.

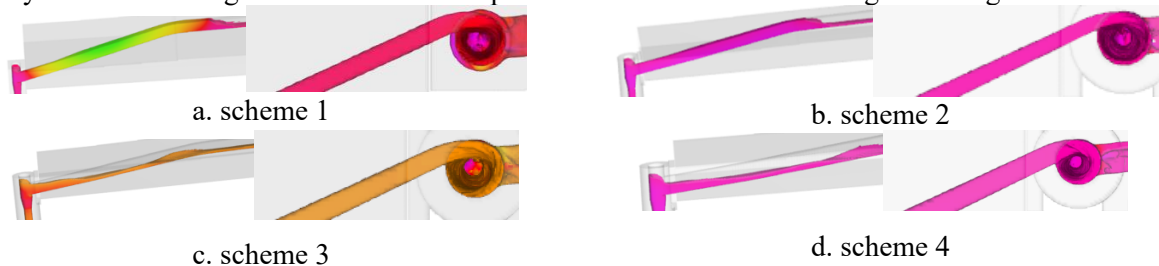


Figure 3. Flow pattern diagram in upstream channel section and volute chamber of each scheme (lateral view).

Table 2. The flow velocity and water surface line of upstream channel section in typical position.

Scheme	Position	Outlet of chute section	Middle of the curve section	Start point of the transition section	End point of the transition section	Entrance of volute chamber
1	Flow velocity ($m \cdot s^{-1}$)	18.0	4.50	3.40	6.31	6.47
	Water surface elevation (m)	1776.366	1775.459	1774.937(Full flow)	1774.762(Full flow)	1774.562(Full flow)
2	Flow velocity ($m \cdot s^{-1}$)	18.0	4.55	3.44	6.45	7.30
	Water surface elevation (m)	1774.316	1775.459	1774.937(Full flow)	1774.762(Full flow)	1774.562(Full flow)
3	Flow velocity ($m \cdot s^{-1}$)	17.5	14.20	11.60	9.26	7.06
	Water surface elevation (m)	1774.236	1774.024	1772.675	1773.524	1774.493
4	Flow velocity ($m \cdot s^{-1}$)	17.9	14.20	11.60	10.82	8.90
	Water surface elevation (m)	1774.196	1774.024	1772.675	1773.282	1773.6

3.3. Flow velocity analysis

Data in Table 2 show the flow velocity and water surface profile along the upstream channel section in different schemes.

In scheme 1, the flow velocity at the outlet of the chute section is 22.50 m/s. The water flow is in a pressure flow pattern before the curve section, and the flow velocity in the middle of the curve section is 4.50m/s, and then the flow velocity decreased gradually. As the width of the transition section changes from 2.0m to 1.0m, the flow velocity increases from 3.40m/s to 6.47m/s at the entrance of the volute chamber. The water flow drains down clockwise in the shaft with velocity of 7.50m/s.

In scheme 2, the flow velocity at the outlet of the chute section is 22.50 m/s. The water flow is in a pressure flow pattern on the middle of the curve section, and the flow velocity in this position is 4.55m/s. After that, the flow velocity is not much different with the scheme 1. Because the diameter of the volute chamber increases, the flow velocity at the entrance of the volute chamber increases to 7.30m /s.

In scheme 3, the flow velocity at the outlet of the chute section is 21.50 m/s. As the width of the entrance section increases, the velocity along the distance increases compared with scheme 2. The water flow drains down clockwise in the shaft with velocity of 7.40m/s.

In scheme 4, as the width of the entrance section increases further, the non-pressure flow pattern appeared before the entrance of the volute chamber, and the flow velocity along the distance increases further compared with scheme 3. However, as the inlet velocity is too large, the flow near the center of the volute chamber directly hits on the wall of the volute chamber, which leads to the instability of the flow pattern in the shaft.

According to the analysis of numerical simulation results, the water flow is spirally moved by the wall of the shaft under the action of gravity, and a cavity is formed in the center of the shaft to maintain the stability of the flow pattern. As the diameter of the volute chamber increases, the pitch of the swirling flow in the volute chamber gradually increases, thereby reducing the compression of the inlet flow, and the length of the pressure flow in the upstream channel section of the shaft is correspondingly reduced. The numerical simulation reveals that the width of the inlet should be kept within the reasonable range of $0.2D \sim 0.4D$ (D is the diameter of the shaft). If the width of the inlet is so small, it will seriously affect the discharge capacity of the swirling shaft. If the width of the inlet is so big, the flow will directly hit the inner wall of the volute chamber, and form the unstable cavity of the volute chamber.

3.4. Energy dissipation rate analysis

In the calculation of the energy dissipation rate of this swirling shaft, the first section is taken at the inlet of the volute chamber, and the inlet of the adit section of the shaft is taken as the second section. The following formula is adopted to calculate the energy dissipation rate:

$$\eta = 1 - \frac{1}{Z} \left(h + \frac{V^2}{2g} \right) \quad (1)$$

In the formula:

Z —The elevation difference between the inlet of the volute chamber and the bottom of the inlet of the adit section;

V —Average flow velocity, $V=0.95V_{\max}$;

h —Average depth of velocity section, $h=Q/(BV)$;

B —Width of section;

Table 3 shows the calculation results.

It can be seen from the above table 3 that the overall energy dissipation rate does not vary significantly with the change of diameter and the entrance section width of the volute chamber. When the diameter of the volute chamber increases from 2.5 m to 3.0 m, the energy dissipation rate increases about 0.89%. As the width of the entrance section increases, the energy dissipation rate increases firstly and then decreases, the overall fluctuation is less than 1%. This indicates that the optimization of the volute chamber and entrance section is less affected the energy dissipation rate.

Table 3. Comparison of energy dissipation rate of different scheme.

Parameter description	Scheme 1	Scheme 2	Scheme 3	Scheme 4
Inlet width (m)	1.0	1.0	1.2	1.5
Velocity at entrance of volute chamber ($\text{m}\cdot\text{s}^{-1}$)	7.80	8.60	7.06	8.90
Velocity at inlet of the adit section ($\text{m}\cdot\text{s}^{-1}$)	9.20	12.50	11.60	11.60
Water depth at inlet of the adit section (m)	1.80	1.65	1.70	1.75
Energy dissipation rate	95.49%	96.38%	97.17%	97.00%

Under the test case scheme 3, the water flow smoothly enters the transition section. The pressure flow is formed 10m before the entrance of the volute chamber. The highest elevation of the water surface in the volute chamber does not exceed the original designed elevation. The water flows tangentially to the volute chamber, and is spiraling downward clockwise to the dissipation well. The overall water flow pattern is smooth. The energy dissipation rate of the overall sluiceway is high. According to the analysis of numerical calculation results, scheme 3 can be adopted as a recommended scheme. The next step is to further verify the rationality of scheme 3 under small flow by combining

with physical model tests and to propose an optimization scheme that can improve the flow pattern at the entrance section of the sluiceway.

4. Physical model results and analysis

In order to ensure that the water depth of the model is larger than 2cm, and the scale of the site is controlled within a certain range, the physical model is conducted according to the 1:25 geometric scale. Under the corresponding test case scheme 3, the water flow pattern is non-pressure flow from chute section to the transition section, and water flow pattern is pressure flow from the start point of the transition section to the entrance of the volute chamber. The water flows into the volute chamber to form a swirling flow, and the highest elevation of the water surface in the volute chamber is 1776.087 m. The diameter of the cavity in the volute chamber is about 1.5m, and the water flow rotates adherence the wall and flows downward, which is basically consistent with the numerical simulation flow pattern. Figure 4 shows the flow pattern of the volute chamber under the designed flow discharge.

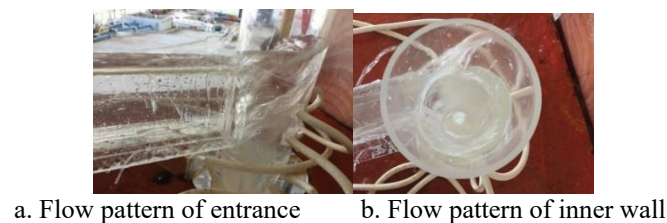


Figure 4. Flow pattern diagram of the volute chamber and inner wall under the flow discharge $20\text{m}^3/\text{s}$.

The comparison of parameters in the representative position under the designed flow discharge of scheme 3 between the numerical simulation and the physical model test has been conducted. Table 4 shows the detail results of comparison.

Table 4. Comparison of physical model test results and numerical simulation results in scheme 3.

Hydraulic parameter description	Scheme 3 (physical model test)	Scheme 3 (numerical simulation)
Entrance width (m)	1.2	1.2
Water depth at the outlet of chute section (m)	0.50	0.67
Velocity at the outlet of chute section ($\text{m}\cdot\text{s}^{-1}$)	18.7	17.5
Velocity at entrance of volute chamber ($\text{m}\cdot\text{s}^{-1}$)	7.80	7.30
Length of pressure flow in upstream channel section	from the start point of the transition section to the entrance of the volute chamber	10m in front of the entrance of the volute chamber
Vortex cavity diameter (m)	1.42	1.50
The highest elevation of the water surface in volute chamber (m)	1776.087	1775.485
Velocity at inlet of the adit section ($\text{m}\cdot\text{s}^{-1}$)	9.40	10.60
Water depth at inlet of the adit section (m)	1.80	1.70
Energy dissipation rate	96.50%	95.60%

The comparison results show that the cavity diameter, water surface line, flow velocity, energy dissipation rate and other results of the physical model and the numerical simulation are similar, which indicates the simulation method that adopted the VOF method is more accurate.

The flow pattern along the distance of physical model test in two test cases are shown below:

At a flow discharge of $5.2\text{m}^3/\text{s}$, the average water depth at the inlet of the volute chamber is 1.12m . At the end of the entrance section, a small part of the water flow tangentially enters the volute chamber to swirl, and most of the water falls directly on the volute chamber wall. The highest elevation of the volute chamber is 1772.212m , and the diameter of the swirling cavity is about 2.6m . Then, through the constraint of the transition section of the volute chamber, it rotates spiraling downward in a clockwise direction to the dissipation well. At a flow discharge of $11.3\text{m}^3/\text{s}$, the average depth of the transition section is 1.30m . The rotating water in the volute chamber meets the incoming water at the entrance of the volute chamber, which results in a significant rising of water level at 1.25m in front of the inlet, with a maximum depth of about 2.12m . After the water enters the volute chamber, most of it can smoothly rotate and flow downward adherence the wall, and a small part of the water directly hits on the wall. The diameter of the swirling cavity in the volute chamber is about 2.0m , and the highest elevation of the water surface in the volute chamber is 1775.712m . Figure 5 shows the flow pattern of the inlet and the inner of the volute chamber at each flow discharge.



a. discharge $5.2\text{m}^3/\text{s}$ (lateral view); b. discharge $5.2\text{m}^3/\text{s}$ (top view); c. discharge $11.3\text{m}^3/\text{s}$ (lateral view); d. discharge $11.3\text{m}^3/\text{s}$ (top view)

Figure 5. Flow pattern diagram of the volute chamber at small flow discharge in scheme 3.

The physical model test results under various flow discharge show that before the water flow enters the shaft, the flow velocity is between 5.00m/s and 23.20m/s , and the maximum flow velocity is about 23.18m/s , which occurs in the chute section. The velocity near the wall is about $2.00\text{--}7.50\text{m/s}$ after the water flows into the volute chamber. The water flow in the middle of the shaft is basically adherent with the inner wall.

5. Research of rectification flip bucket

5.1. Arrangement of arc wedge-shaped rectification flip bucket

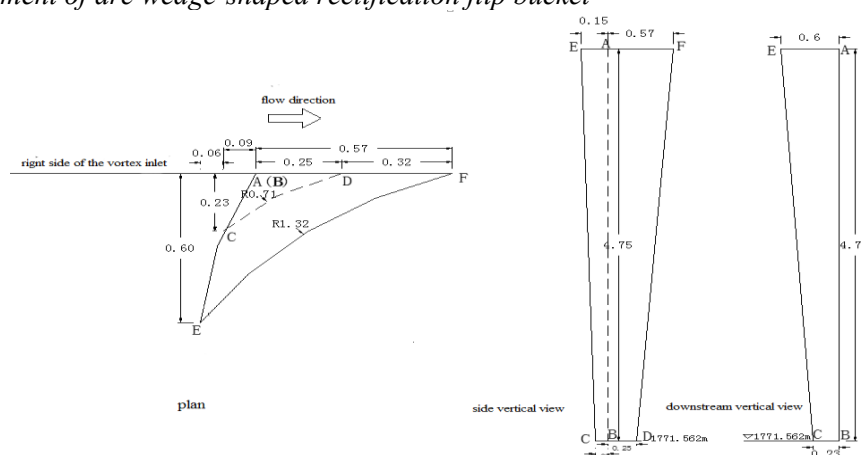


Figure 6. Schematic diagram of rectification flip bucket in volute chamber.

From the results of numerical simulation and physical model test, it indicates the flow pattern of the scheme 3 is the relatively stable one in 4 test cases. But under this scheme, the swirling of water flow in the volute chamber is not perfect at small flow discharge, and the entrance section of the volute chamber is still close to full section flow pattern at designed discharge, which needs further

optimization. Through theoretical analysis and reference to the existing research results, it is proposed to set the rectification flip bucket at the inlet of volute chamber, to solve the problem that the raising water level of entrance section occurred at designed discharge and the water flow cannot swirl successfully adherent with the inner wall at small flow discharge. In the physical model test, the selection of the arc wedge-shaped rectification flip bucket has been tested several times. Through the different combinations of height, width, type and arrangement method, a better arc wedge-shaped rectification flip bucket has been selected finally. The rectification flip bucket is set at the inlet and attached to the right-side wall of the volute chamber. The bottom elevation is the same as the inlet: 1771.562m, the top elevation is flush with the right-side wall of the inlet: 1776.312m. Figure 6 shows the layout of the arc wedge-shaped rectification flip bucket.

5.2. Model test results of rectification flip bucket



a. discharge 5.2 m³/s ; b. discharge 11.3 m³/s



a. Flow pattern of lateral view; b. Flow pattern of top view

Figure 7. Flow pattern of the volute chamber of lower discharge (top view).

Figure 8. Flow pattern of the volute chamber of discharge 20 m³/s.

Table 5. The flow velocity and the water surface line in the scheme with the rectification flip bucket

Position	Station number(m)	Q=5.2 m ³ ·s ⁻¹		Q=11.3 m ³ ·s ⁻¹				Q=20 m ³ ·s ⁻¹					
		Water depth (m)		Flow velocity (m·s ⁻¹)		Water depth (m)		Flow velocity (m·s ⁻¹)		Water depth (m)		Flow velocity (m·s ⁻¹)	
		Left	Right	Left	Right	Left	Right	Left	Right	Left	Right	Left	Right
Start point of the transition section	0+149.70	1.78	1.68	4.88	6.83	0.63	1	10.05	9.76	1.08	0.93	13.41	12.54
Middle point of the transition section	0+158.70	1.5	1.5	2.96	4.51	1.25	1.25	8.05	9.57	2.5	1.63	9.69	10.58
End point of the transition section	0+168.70	1.5	1.5	4.12	5.23	1.5	1.5	7.1	8.39	3.25	3	8.83	8.81
Inner wall of volute chamber	0+170.50	-	-	4.98	3.66	-	-	7.87	4.49	-	-	5.76	4.78
The starting point of the adit section	0+180.00	0.48	0.55	6.35	6.21	0.88	0.93	7.69	7.85	1.25	1.13	9.23	10.13

5.2.1. Analysis of flow pattern along the distance. During the test, after the rectification flip bucket was adopted, it was found that under the test case with discharge 5.2m³/s, the water tangentially flows to the volute chamber (Figure 7a), and then through the contraction of the volute chamber, it rotates clockwise and the water flow in the shaft is basically adherent the wall; under the test case with discharge 11.3m³/s, the water flow the swirling flow is formed in the shaft, and there is no obvious rising of water level at the entrance of the volute chamber (Figure 7b); under the test case with discharge 20m³/s, a entrained-air flow is formed 5m in front of the inlet of the volute chamber. The water flow pattern is non-pressure flow (Figure 8a). In addition, the lower part of the arc wedge-shaped rectification flip bucket retracts so that it does not squeeze the lower flow from the inlet, and the upper part drives the upper layer water to accelerate the swirling adherence the inner wall of the volute chamber. From the perspective of the overall flow pattern of the swirling shaft, the venting cavity in the volute chamber and the shaft is stable, and the flow pattern is greatly improved compared with the scheme 3 (see Figure 8b).

5.2.2. *Surface line, flow velocity and energy dissipation rate.* Table 5 shows the specific data of these parameters.

6. Conclusions

Based on a project of water diversion in Yunnan, this paper combines numerical simulation and physical model test to study the flow characteristics and energy dissipation rate of the swirling shaft by adjusting the diameter and the width of the inlet of the volute chamber. Besides that, a further analyze of the arrangement of the rectification flip bucket has been conducted, and a more reasonable volute chamber body shape for solving practical engineering problems has been recommended finally. This paper can draw the following conclusions through research and analysis:

(1) The modified RNG k- ε turbulence model based on VOF method can simulate the water flow in swirling shaft with characteristics of strong rotational flow and anisotropy. The flow pattern and distribution of velocity in swirling shaft can be obtained by numerical simulation.

(2) Numerical simulation studies have found that with the diameter of the volute chamber increases, the pitch of the swirling flow in the volute chamber gradually increases, thereby reducing the compression of the inlet flow, and the length of the pressure flow in the upstream channel section of the shaft is correspondingly reduced.

(3) Numerical simulation studies have found that the width of the inlet of the volute chamber should be kept within the reasonable range of 0.2D-0.4D (D is the diameter of the shaft).

(4) Physical model test results reveal that, after adopted arc wedge-shaped rectification flip bucket on the inner wall of the volute chamber, the swirling flow in the volute chamber can intersect with the inlet flow at a certain angle to avoid direct collision in the entrance, which can change the flow pattern of the upstream channel section of the shaft from pressure flow to non-pressure and effectively improve the flow pattern in the volute chamber.

References

- [1] Xiao Baiyun 2001 Research on Large-flow Discharge and Energy Dissipation Technology of High Arch Dam of Xiluodu Hydropower Station [J] *Water Power* **08** 69-71
- [2] Nan Junhu, Niu Zhengming, Hong Di, et al. 2013 Study on Hydraulic Characteristics of Horizontal Borehole Spillway Tunnel in Gongboxia [J] *Journal of Hydroelectric Engineering* **03** 101-107
- [3] Shao Jingdong 2003 Application of Swirling Shaft Flood Discharge Tunnel in Shapai Engineering [J] *Design of Hydroelectric Power Station* **04** 61-63
- [4] Gao Jizhang, Dong Xinglin, Liu Jiguang 2008 Eco-environmentally Friendly Energy Dissipation Technology - Research and Application of Internal Energy Dissipation [J] *Journal of Hydraulic Engineering* **10** 1176-1182
- [5] Drioli C 1969 Esperienze su installazio ni con pozzo di scarico a Vortice [J] *L'Energia Elettrica*. 6
- [6] Jeanpierre D, Lachal A. Dissipation d energie dans un puits a vorte[M]. *La Houille Blance* 7 1966.
- [7] Qian Xiaoyan, Deng Jun, Zhang Yelin, et al. 2011 Test and Numerical Simulation of Rectifier Rectifier in Shaft Swirl and Spillway Tunnel [J] *Yangtze River* **11** 20-22
- [8] Dong Xinglin, Guo Jun, Yang Kailin, et al. 2003 Research Progress on Energy Dissipator in High Water Head Large Flow Discharge Tunnel [J] *Journal of China Institute of Water Resources and Hydropower Research* **03** 21-25
- [9] Gou Fangrong, Huang Huang 2003 [J] *Sichuan Water Power* **04** 31-33
- [10] Chen Huayong, Deng Jun, Hu Jing, et al. 2008 [J] *Water Power* **03** 79-82
- [11] Cao Shuangli, Niu Zhengming, et al. 2009 [J] *Xi'an University of Technology* **25(3)** 263-269
- [12] Chen Dahong, Chen Wei 2005 [J] *Engineering Journal of Wuhan University* **38(5)** 54-56
- [13] Zhang Xiaodong ,Liu Zhiping, Gao Jizhang, Wang Xiaosong 2003 [J] *Journal of Hydraulic Engineering* **08** 58-63